Baghdad Science Journal

Volume 23 | Issue 6 Article 15

6-22-2026

Synthesis and Characterization of Zinc Oxide (ZnO) Nanoparticles: From Chemical to Green Synthesis

Kawa S. Sulaiman
Department of Physics, College of Education, Salahaddin University-Erbil, Erbil, Iraq, kawa.sulaiman@su.edu.krd

Ayoub S. Karim
Department of Physics, College of Education, Salahaddin University-Erbil, Erbil, Iraq, ayoub.karim@su.edu.krd

How to Cite this Article

Sulaiman, Kawa S. and Karim, Ayoub S. (2026) "Synthesis and Characterization of Zinc Oxide (ZnO) Nanoparticles: From Chemical to Green Synthesis," *Baghdad Science Journal*: Vol. 23: Iss. 6, Article 15.
DOI: https://doi.org/10.21123/2411-7986.5329

BAGHDAD SCIENCE JOURNAL 2026;23(6):2143–2154

RESEARCH ARTICLE

Synthesis and Characterization of Zinc Oxide (ZnO) Nanoparticles: From Chemical to Green Synthesis

Kawa S. Sulaiman *, **Ayoub S. Karim**

Department of Physics, College of Education, Salahaddin University-Erbil, Erbil, Iraq

ABSTRACT

The present research focuses on the synthesis and comparative analysis of zinc oxide nanoparticles (ZnO NPs) produced through two distinct methodologies: a traditional sol-gel procedure and a sustainable green synthesis route. The green synthesis approach utilized Laurus Nobilis leaf extract as a natural reducing and stabilizing agent, offering an eco-friendly alternative to conventional chemical synthesis. To evaluate the structural, optical, and morphological properties of the resulting nanoparticles, both sets of samples were characterized using UV-Vis spectroscopy, XRD, energy-dispersive X-ray spectroscopy (EDX), FTIR, and Field Emission Scanning Electron Microscopy (FESEM). The XRD patterns confirmed the successful formation of a hexagonal wurtzite structure in both samples, indicating high crystallinity. The average crystalline size was calculated to be 25.77 nm for the sol-gel approach and 18.46 nm for the green synthesis. UV-Vis spectroscopy was employed to investigate the optical characteristics, revealing average band gaps of 2.84 eV for the sol-gel method and 2.81 eV for the green method. Furthermore, EDX characterization demonstrated that the ZnO NPs possessed high elemental purity; the sol-gel method resulted in 80.9% zinc and 19.1% oxygen, while the green method yielded a composition of 81% zinc and 19% oxygen. Morphological analysis via FESEM micrographs revealed a significant difference in particle shape: the sol-gel method produced nano-rice or nano-rod formations with an average size of 173 nm, whereas the green technique produced predominantly spherical nanoparticles with an average size of 151 nm. These results highlight the effectiveness of both methods in producing high-quality metal oxide nanoparticles with controllable physical properties.

Keywords: Characterization, Green synthesis, Laurus nobilis, Sol-gel method, ZnO nanoparticles

Introduction

Nanotechnology is a multidisciplinary field centered on the engineering and manipulation of structures and devices at the atomic and molecular scale, typically under 100 nanometers. Its significance stems from its capacity for atomic-level control, which enables transformative applications across electronics, optics, optoelectronics, and biology, including targeted gene delivery and the enhancement of radiological therapies.[1] There are three methods for producing nanoparticles: physical, chemical, and biological. Although physical and chemical processes have traditionally been used to create nanoparticles, they are hazardous to the environment since they need a lot of energy and dangerous materials.[2] An eco-friendly substitute for conventional synthesis methods has been made possible by green synthesis technologies, especially plant-mediated processes. These techniques have employed biomolecules, microbes, or plant extracts to stabilize nanoparticles and lower metal ions. One major area of nanotechnology advancement at the moment is the creation of nanoparticles in

Received 18 August 2025; revised 23 April 2026; accepted 26 April 2026.
Available online 22 June 2026

* Corresponding Author.
E-mail addresses: kawa.sulaiman@su.edu.krd (K. S. Sulaiman), ayoub.karim@su.edu.krd (A. S. Karim).

https://doi.org/10.21123/2411-7986.5329

a more environmentally friendly and bio-based manner.[3]

Zinc oxide (ZnO)—an inorganic semiconductor with a hexagonal wurtzite structure—has a large band gap (3.37 eV) and a high exciton binding energy (60 meV), making it very promising.[4,5]

Nanoparticles made of zinc oxide (ZnO NPs) have several useful characteristics, such as being transparent to light, conducting electricity, piezoelectric, biocompatible, inexpensive, abundant in nature, and long-lasting.[6,7] They are employed in many different fields, including laser and optoelectronic devices, paints, varnishes, polymers, solar cells, gas sensors, catalysis, and medications.[8,9] Numerous applications for these particles exist, such as medication delivery, filtration, tumor heating, nanocomposites, and medical imaging.[10,11]

There are different ways to make ZnO-NPs of different sizes, such as using solvothermal and hydrothermal synthesis,[12] precipitation[13] polymerization method,[14] laser ablation[15] sonochemical[16,17] chemical vapor deposition,[18] thermal decomposition[19] and sol-gel.[20] Because the sol-gel method enables controlled consolidation, shape change, nanostructure patterning, and low processing temperatures, researchers are very interested in it.[21] Numerous investigations examine the biosynthesis of ZnO NPs utilizing various natural plant extracts. The findings show that the samples' properties change depending on the plant extract source used.[22,23] In the literature review Table 1, recent studies on ZnO NPs synthesized using different plant extracts are summarized. Additionally, the sol–gel method has also been widely used for the synthesis of ZnO NPs, and several studies provide comparisons between these two approaches.

The novelty of the present study is the synthesis of ZnO NPs via two distinct methods, namely a sol–gel technique and a green route using Laurus nobilis leaf extract. A systematic comparison of the structural, morphological, compositional, and optical properties of the obtained nanoparticles is performed. To the best of our knowledge, this is the first study reporting the use of Laurus nobilis extract for ZnO NP synthesis and its direct comparison with the sol–gel method.

Materials and methods

Chemical use

In this work, zinc acetate dehydrate ($ZnC_4H_6O_{4.2}H_2O$), ethylamine (C_2H_2N), ethanol (C_2H_5OH), sodium hydroxide (NaOH) from Schallab S.L., Spain, and deionized water were all acquired from RIEDEL-DE-HAEN AG.

Preparation of plant extract

Laurus nobilis, commonly known as the bay laurel, is a native evergreen shrub or tree of the

Table 1. Literature review of recent studies on ZnO NPs.

Synthesis method	Precursor type	Reducing and stabilizing agent	Morphology of NPs	References
Sol-gel	Zinc nitrate	NaOH	Spherical shape	24
Green	Zinc nitrate	Brassicaceate seed extract	Spherical shape	
Sol-gel	Zinc nitrate hexahydrate	Arabic gum	Spherical, uniform	25
Chemical: Wet precipitation	Chemical: Zinc nitrate	hexahydrate + NaOH	spherical	26
Green: Marine alga	Green: Zinc acetate dehydrate	Ulva fasciata aqueous extract	rod-shaped	
Green: Ultrasonication-assisted	Zinc acetate dihydrate + NaOH (pH adj.)	Laura's Nobili's L. leaf extract	Hexagonal, homogeneous,	27
Green	Zinc acetate dihydrate + NaOH (pH 12)	Laura's Nobili's leaf extract	Roughly spherical	28
Green: Co-precipitation	$Zn(OAc)\cdot 2H_2O$ and $Zn(NO_3)_2\cdot 6H_2O$ (two batches)	Laura's Nobili's L. leaf extract	Acetate: bullet-shaped Nitrate: flower-shaped	29
Sol-gel: Review	Zinc acetate dehydrate, zinc chloride; solvent: ethanol	NaOH or monoethanolamine	Spherical,rod-like	30
Green	$Zn(NO_3)_2\cdot 6H_2O$ + NaOH (pH adj.)	Pinus brutia leaf extract (flavonoids, glycosides, polyphenols, terpenoids)	Spherical	31
Sol-gel	Zinc acetate ($C_4H_6O_4Zn\cdot 2H_2O$) in ethanol + NaOH	NaOH (pH controller)	Nano flake (flat, irregular);	32
Green	$Zn(NO_3)_2\cdot 6H_2O$	Laura's Nobili's extract	Spherical	33
Green: Multiple plants	Zinc acetate or zinc nitrate (study-dependent)	Various: A. indica, L. nobilis, S. torvum, C. pictus extracts; Aeromonas hydrophila; Bacillus megaterium	Mostly spherical, nanorods	34

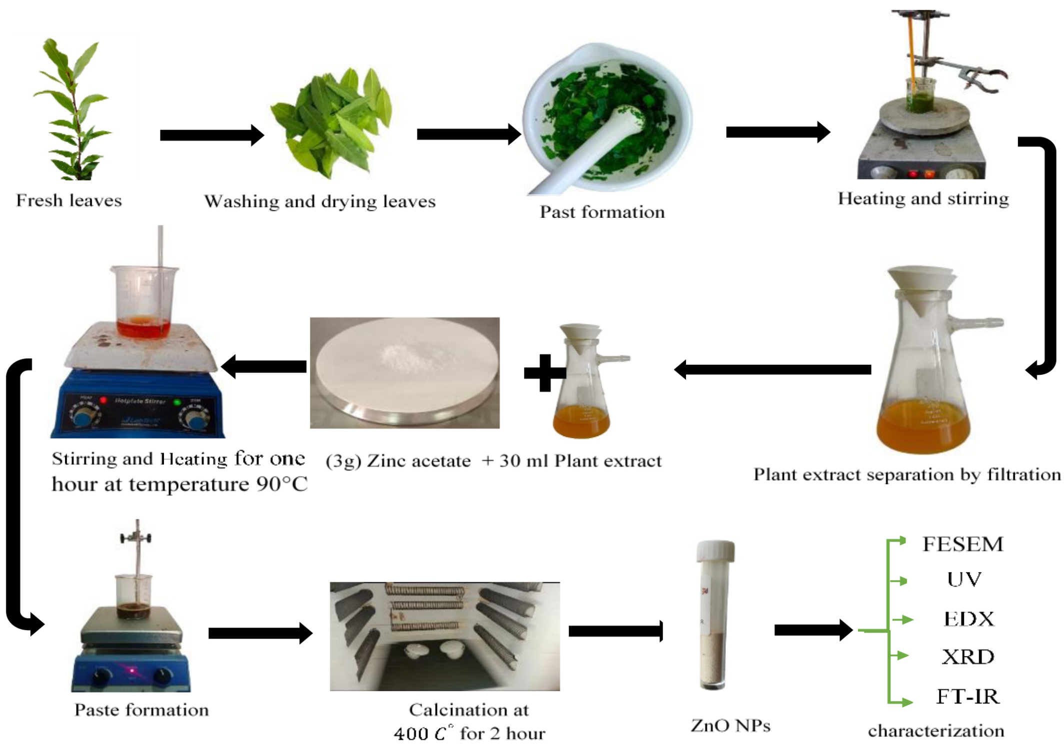

Fig. 1. Schematic diagram representation of the leaf extracts of the LN and ZnO NPs preparation green method.

Mediterranean region. It is now cultivated globally as an ornamental plant and for its aromatic leaves, with significant presence in southern Europe, western Asia, northern Africa, and the Americas. Nobili leaves were collected from the Akre-Gulan region, which is located at 36°43’49.4"N 43°53’10.7"E. Fresh Laurus nobilis leaves were cleansed multiple times using both tap water and de-ionized water to remove any excess dirt. Subsequently, the leaves were reduced to small pieces by cutting them. The small pieces were then crushed using a pestle and mortar to form a paste. After adding 100 ml of distilled water to the paste, the mixture was heated at 70°C for 45 minutes while being agitated with a magnetic stirrer at 600 r.p.m. Once the extract had been filtered through Whatmann No. 1 paper, it was allowed to cool to ambient temperature. Fig. 1 shows the steps used to get the clear liquid extract, which included centrifugation, filtering, and low-temperature storage in the refrigerator for use in subsequent studies.

Preparation of ZnO NPs

Green synthesis of ZnO NPs

In the green synthesis, 3 g of zinc acetate dihydrate powder was combined with 30 mL of Laurus Nobilis leaf extract. The mixture was heated to 90°C under constant stirring using a magnetic hotplate. A 1M sodium hydroxide (NaOH) solution was then added dropwise to the mixture until a yellow coloration appeared and the pH stabilized at 9. Heating and stirring were continued at this temperature until the mixture condensed into a thick paste. The resulting paste was transferred to an air oven and dried at 90°C for one hour. The solid product was then repeatedly washed with distilled water to remove any residual basic compounds. Finally, the sample was calcined at 400°C for two hours and stored in a desiccator to prevent moisture absorption.

Sol-gel method of ZnO NPs

One hundred milliliters of 0.2M zinc acetate hydrate (4.3898 g) is combined with fifty milliliters of ethanol and fifty milliliters of ethylamine ($C_2H_5NH_2$) as a stabilizer, then mixed using a magnetic stirrer for ten minutes. Subsequently, the solution is stirred at 70°C for two hours, as depicted in Fig. 2. After cooling to room temperature, one hundred milliliters of distilled water is added dropwise using a burette, resulting in precipitate formation. Whatman No. 1 filter paper is used to filter the precipitate, as illustrated in Fig. 2, and then dried for four hours in a hot air oven at 100°C. Finally, the material undergoes annealing and calcination at 500°C for one hour. The zinc oxide nanoparticle (ZnO NPs) sample is prepared for characterization.

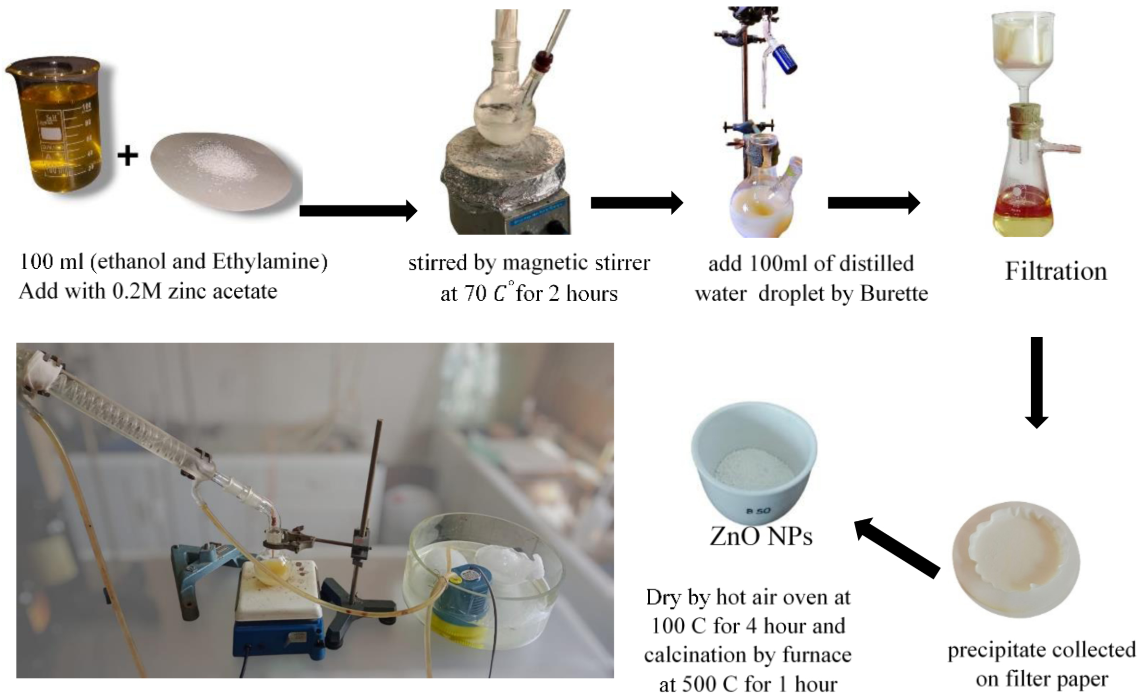

Fig. 2. Setup and schematic diagram representation of ZnO NPs by the sol-gel method.

Results and discussion

Characterization of LN leaf extract

UV-Visible analysis of LN leaf extract

The UV-visible spectrum of extracts from the leaf of the LN plant is displayed in Fig. 3. The wavelength at which a maximum peak was seen was 280 nm. Because OH groups are common stabilizing agents, it is conceivable that the phytochemicals found in the extracts of Laurus Nobilis leaves are responsible for the observed peak. It is possible to use bio-reducing to create nanoparticles. [35]

The leaves of Laurus Nobilis are a significant resource for nanoparticle synthesis because of their bioactive chemicals, which aid in the reduction, stability, and functionalization of nanoparticles, as well as possessing intrinsic medicinal characteristics. [36] Due to their antioxidant properties and lack of toxic substances, these phytochemicals continue to be effective in reducing metal ions and stabilizing them at the nanoscale. Furthermore, phytochemicals have the ability to generate nanoparticles of diverse sizes and forms. [37]

FTIR analysis of LN leaf extract

Infrared Fourier Transform Spectroscopy (FTIR) was used to study the functional groups of reductive biomolecules and their role in the reduction and stabilization of ZnO NPs in plant extracts. [38,39] The FTIR spectrum of the leaves of Laurus Nobilis extracts is presented in Fig. 3 above. It is evident that the FTIR spectrum displays several peaks within the range of 400 to 4000 cm^{-1}. The FTIR spectrum can be categorized into two distinct regions. The first region, ranging from 0 to 1500 cm^{-1}, is referred to as the fingerprint region. In this area, it is evident that the plant extract can be utilized for the production of ZnO nanoparticles. The functional group region spans from 1800 to 4000 cm^{-1}. FTIR spectra provide insights into the characteristics of material bonding across all states of matter. [40,41]

Commonly associated with carbs or phenolic chemicals is the absorption peak at 1207.2 cm^{-1}, which is caused by C-O bonds. [42] Carboxylic acids, esters, aldehydes, and ketones all have a characteristic absorption band at 1635 cm^{-1}. [42] The aromatic primary amine and NH stretch are shown by the peak at 3452 cm^{-1}. [43] The O-H stretching vibration at 3350 cm^{-1} and the C-H out-of-plane bending band at 599.76 cm^{-1} are both picked up by the peak. [44]

It is confirmed that the leaf extract contains phenolic chemicals since the FTIR spectrum shows a strong peak at 3425 cm^{-1}, which corresponds to the stretching of the OH group. Amino acid stretching frequencies are correlated with the infrared stretching frequency at 2096 cm^{-1}.

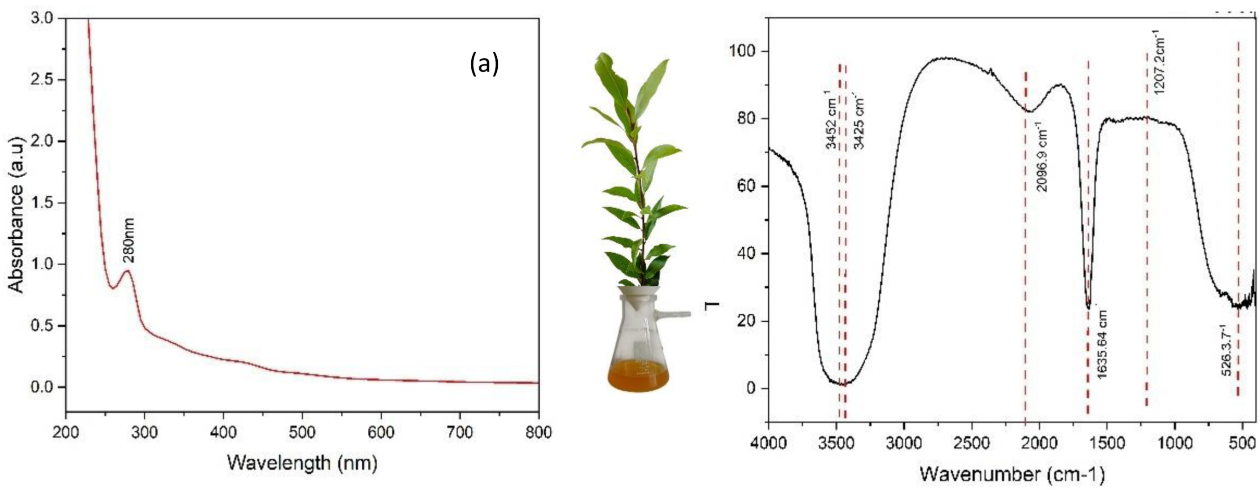

Fig. 3. (a) UV-Visible absorption spectrum and (b) FTIR spectrum of LN leaf extract.

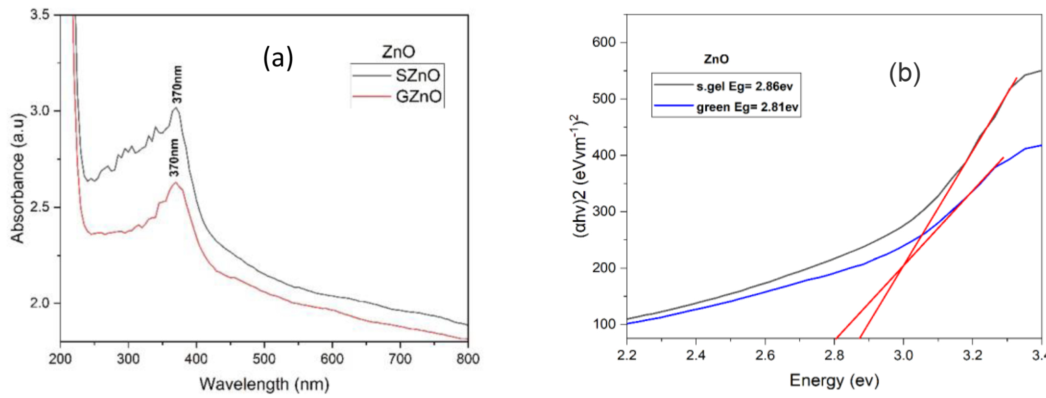

Fig. 4. (a) UV-visible absorption spectra sol-gel and green methods synthesis ZnO NPs (b) Tauc plots $(\alpha h\nu)2$ versus $h\nu$ of ZnO NPs.

Characterizations of ZnO NPs

Optical analysis of ZnO NPs

UV-Visible spectrum of ZnO NPs

Utilizing UV-Vis spectrophotometry, the optical properties of ZnO nanoparticles were investigated. produced using sol-gel and green techniques. Both samples exhibited a characteristic absorption peak at 370 nm, as shown in Fig. 4 (a), which corresponds to ZnO's intrinsic bandgap absorption brought on by valence-to-conduction band electron transitions. The Tauc plot relation, expressed by Eq. (1), was used to calculate the optical band gap[45]

$$\alpha h\vartheta = A\left(h\vartheta - E_g\right)^{\gamma} \quad (1)$$

In this context, α represents the optical absorption coefficient, A is a constant referred to as the band tailing parameter, $h\upsilon$ symbolizes the energy in electron volts (eV), Eg signifies the energy band gap of the material, and γ is the exponent parameter. For a direct permitted transition, γ it is equal to two.

The green-synthesized ZnO NPs have a value of 2.80 eV, and the sol-gel-derived ZnO NPs have a value of 2.84 eV, as seen in Fig. 4. The small discrepancies in bandgap energies could be due to variations in particle size, crystallinity, or surface imperfections caused by how the particles were made. The absorption peaks at 370 nm and the bandgap values that are quite close to each other show that both approaches make ZnO NPs with similar electrical structures. The bandgap of green-synthesized ZnO NPs (2.80 eV) is slightly lower than that of sol-gel NPs (2.84 eV). This could mean that quantum confinement effects are slightly weaker, possibly because the particles are slightly larger or the surface has changed due to the organic phytochemicals used in the green approach.[46] Although these two processes differ slightly, both produce ZnO NPs with optimal semiconductor characteristics for photocatalytic and optoelectronic applications.

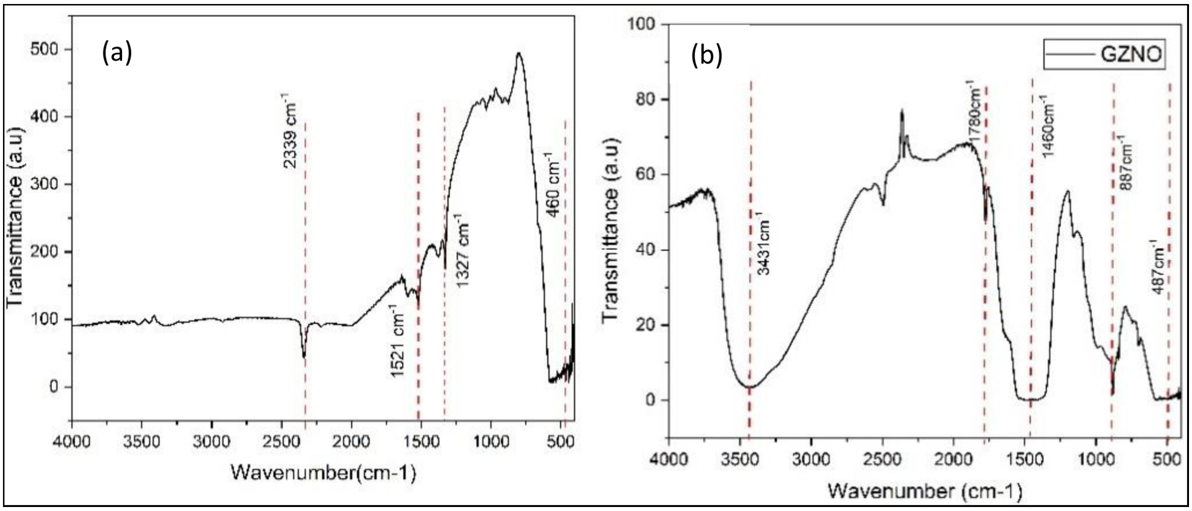

Fig. 5. (a) FTIR spectrum of ZnO NPs for the sol-gel method and (b) FTIR ZnO NPs for green-method synthesis.

FTIR spectrum of ZnO NPs

Fig. 5(a) illustrates the FTIR spectrum of ZnO nanoparticles synthesized by the sol-gel method. The absorption band at 2339 cm^{-1}, within the range of 2300 to 2400 cm^{-1}, is attributable to the presence of CO_2 in the atmosphere.[47] The ZnO peak at 460 cm^{-1} in the range of 578 cm^{-1}-420 cm^{-1} indicates that the transition of Zn(OH)2 to ZnO is complete. Previous research discovered the ZnO peak between 464 and 419 cm^{-1}.[48] The peaks at 1521 cm^{-1} and 1327 cm^{-1} correspond to asymmetric and symmetric C=O bond vibrations, respectively.[49,50]

The FTIR spectrum of the green-synthesized ZnO nanoparticles is shown in Fig. 5. At 3431, the most fundamental vibrational mode is the O-H stretching vibration. The prominent peak at 887 cm^{-1} confirmed the presence of a C-H bend in the alkane group. A strong and distinct band at 1460 cm^{-1} indicates the presence of aromatic groups' C-C stretching, while a peak at 1780 cm^{-1} could indicate aromatic rings' C=C stretching, amines' N-H vibration, and carboxylic and amide groups' C=O stretching. The stretching vibrations of ZnO nanoparticles are shown by the signal at 487 cm^{-1}, which is similar to those previously described.[5]

Structural analysis of ZnO NPs

XRD analysis

The use of X-ray diffraction (XRD) provided evidence that the ZnO nanoparticles that were manufactured displayed a crystalline phase that was in agreement with the conventional hexagonal wurtzite structure.

The Debye–Scherrer formula, expressed by Eq. (2), was utilized to calculate the crystallite sizes of both as-prepared and calcined Ln–ZnO NPs using the X-ray line-broadening technique.[51]

$$D = \frac{k\lambda}{\beta cos\theta} \quad (2)$$

In this context, D represents the crystallite size measured in nanometers. The constant k, known as Scherrer's constant, is valued at 0.94. With a value of 1.54178 Å, the X-ray wavelength is represented by λ. The Bragg angle is represented by θ, and the word β is the full width at half maximum (FWHM) of the peak.

The XRD analysis of ZnO NPs using the sol-gel technique reveals a zincite phase with a hexagonal wurtzite crystal structure and lattice constants of a = b = 3.249Å and c = 5.206Å. The diffraction peaks were found at θ = (31.777°), (34.426°), (36.262°), (47.549°), (56.611°), (62.869°), (66.396°), (67.965°), (69.106°), (72.577°), and (76.981°), These peaks are indexed as (100), (002), (101), (102), (110), (103), (200), (112), (201), (004) and (202) diffraction lattice planes, as illustrated in Fig. 6, to compute the crystal size using the Debye-Scherrer formula, the crystal size is equal (25.77 nm).

XRD analysis for ZnO nanoparticles via green synthesis is presented in Fig. 6. The diffraction peaks of the nanoparticles are recognized as belonging to the zincite phase, characterized by a hexagonal wurtzite crystal structure, with lattice constants of a = b = 3.2200 Å and c = 5.2000 Å. The diffraction peaks were found at θ = (32.071°), (34.467°), (36.534°), (47.791°), (57.168°), (63.102°), (67.072°), (68.492°), (69.777°), (72.675°), and (77.642°), These peaks are indexed as (100), (002), (101), (102), (110), (103), (200), (112), (201), (004), and (202). The diffraction lattice planes, as illustrated in the figure, indicate that the formation of ZnO has

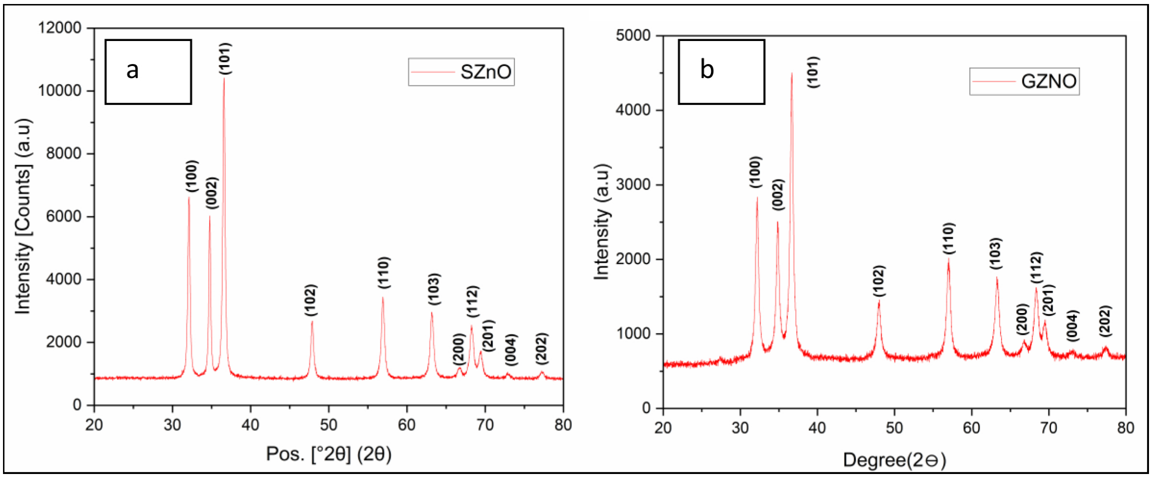

Fig. 6. XRD patterns of ZnO nanoparticles (a) sol-gel method (b) green method.

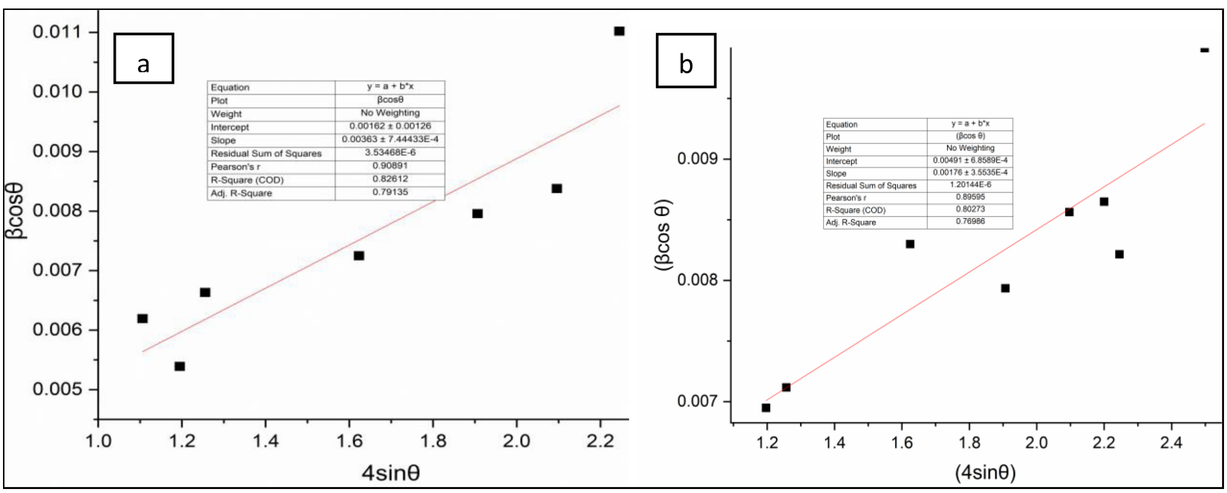

Fig. 7. W-H plot for ZnO nanoparticles (a) sol-gel method (b) green synthesis.

occurred.[44] The synthesized and calcined ZnO had crystallite diameters of 18.46 nm.[52]

The interplanar spacing (d_{hkl}) for both the green synthesis and sol-gel methods was calculated using Eq. (3), based on Bragg's law:

$$d_{hkl} = \frac{\lambda}{2\ sin\theta} \tag{3}$$

where d is the interplanar spacing (Å), λ is the X-ray wavelength of Cu $K\alpha$ radiation equal to 1.54178 Å, θ is the Bragg diffraction angle, and n is the order of reflection, which is taken as unity (n = 1). The interplanar spacing (d) values calculated from Bragg's law for both the green synthesis and sol-gel methods are summarized in Table 2 for the three most intense peaks. The results agree with the standard values from JCPDS Reference code: 96-230-0451.

The crystallite size and microstrain of the synthesized samples were estimated using the Williamson–Hall (W–H) method according to Eq. (4):

$$\beta cos\theta = \frac{k\lambda}{D} + 4\epsilon sin\theta \tag{4}$$

where β is the full width at half maximum, θ is the Bragg angle, k is the shape factor, λ is the X-ray wavelength, D is the crystallite size, and $\epsilon$is the macrostrain. For the sol–gel sample Fig. 7, the macrostrain

Table 2. Interplanar spacing (d_{hkl}) for the first three observed peaks for both methods.

Methods	Miller indices	Observed 2θ	d_{hkl}
Sole-Gel	(100)	31.77	2.8143
	(002)	34.42	2.6035
	(101)	36.26	2.4755
Green	(100)	32.07	2.7887
	(002)	34.46	2.6035
	(101)	36.53	2.4578

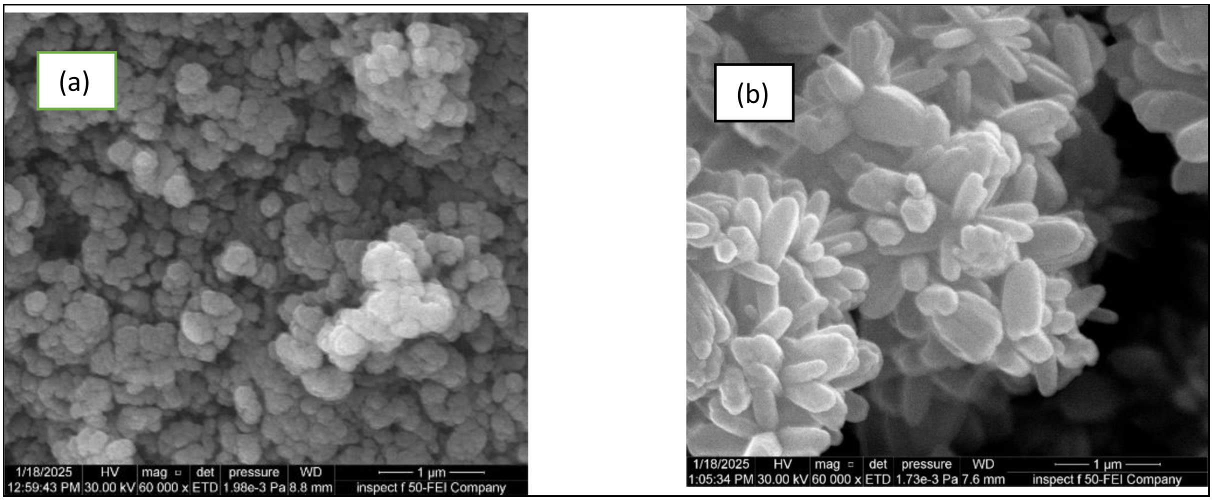

Fig. 8. FESEM image of GS ZnO nanoparticles (a) green method (b) sol-gel method.

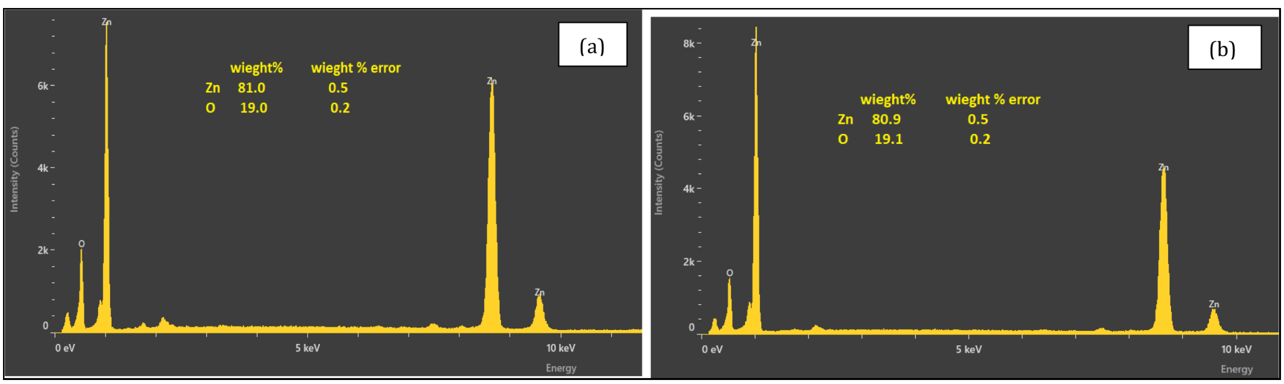

Fig. 9. EDX analysis of GS ZnO nanoparticles (a) green method (b) sol-gel method.

was 0.00363 with an intercept of 0.00162, corresponding to a crystallite size of 85.5 nm. In contrast, the green-synthesized sample Fig. 7 exhibited a lower macrostrain of 0.00176 and an intercept of 0.00491, yielding a smaller crystallite size of 28.23 nm. These results indicate that the synthesis route significantly influences the structural parameters of the obtained nanoparticles.

Morphological and compositional analysis of ZnO NPs

FESEM analysis

Fig. 8 presents FE-SEM images illustrating the surface morphology and topographical analysis of green-produced ZnO nanoparticles utilizing Laurus nobilis L. leaf extract. FESEM images elucidate the distribution, morphology, and dimensions of nanoparticles in the research, facilitating data evaluation and further analysis.[53] The image of green synthesis indicates that all generated nanoparticles have a spherical morphology, as depicted in Fig. 8, which closely aligns with findings from other researchers' studies.[54,55] The average particle size for green synthesis is 151 nm.[56] However, in the sol-gel technique, the morphology of the particles is different. The image depicts a nano-rice or nano-rod shape, as illustrated in Fig. 8, with an average nanoparticle size of 173 nm.

EDX analysis

The chemical compositions of GS ZnO NPs were examined using EDX spectroscopy. The EDX or EDS inspection, as illustrated in Fig. 9, confirms the presence of zinc (Zn) and oxygen (O) elements, ruling out the presence of any defect signals with EDS limits that are connected to the orientation of the feature structures of the GS ZnO NPs.[38]

The EDX results showed that both synthesis procedures successfully generated nanoparticles that included zinc oxide (ZnO). The spectrum had significant peaks for zinc at around 1 keV and 8.75 keV, as well as a clear peak for oxygen at 0.5 keV. These are the main characteristics of ZnO.[43]

Conclusion

In this study, ZnO NPs were successfully synthesized using two different methods: a sol–gel method and a green route employing Laurus nobilis leaf extract. FTIR and UV–Vis spectroscopy were used to investigate the optical properties of the synthesized nanoparticles. The characteristic Zn–O stretching vibration was observed at 487 cm^{-1} for the green-synthesis ZnO NPs, while it appeared in the range of 419–464 cm^{-1} for the sol–gel samples. The estimated band gap energies were 2.81 eV and 2.84 eV for the green and sol–gel methods, respectively. XRD analysis revealed average crystallite sizes of 18.46 nm (for the green method) and 25.77 nm (for the sol–gel method). FESEM analysis showed that the green-synthesized ZnO NPs exhibited a predominantly spherical morphology with an average particle size of 151 nm. In contrast, the sol–gel method produced nanorice or nanorod-like structures with an average size of 173 nm.

Authors' declaration

- Conflicts of Interest: None.
- We hereby confirm that all the Figures and Tables in the manuscript are ours. Furthermore, any Figures and images that are not ours have been included with the necessary permission for re-publication, which is attached to the manuscript.
- No animal studies are present in the manuscript.
- No human studies are present in the manuscript.
- Ethical Clearance: The project was approved by the local ethical committee at Salahaddin University.

Authors' contributions statement

K.S.S Conceptualization, Data curation, Formal analysis, Investigation, Resources, Writing–original draft, Methodology, Visualization, Writing–review & editing. A.S.K Conceptualization, Data curation, Formal analysis, Supervision, Visualization, Writing–review & editing.

References

1. Oleiwi HF, Rahma AJ, Salih SI, Beddai AA. Comparative Study of Sol-Gel and Green Synthesis Technique Using Orange Peel Extract to Prepare TiO_2 Nanoparticles. Baghdad Sci J. 2024;21(5). https://doi.org/10.21123/bsj.2023.8089.
2. Kumar T, Phogat P, Sahgal V, Jha R. Surfactant-mediated modulation of morphology and charge transfer dynamics in tungsten oxide nanoparticles. Phys Scr. 2023;98(8):085936. https://doi.org/10.1088/1402-4896/ace566.
3. Parveen S, Riyazur Rahman F, Thulasi Krishnan S, Kalaiarasi G, Dinesh A, Srimathi Priya L, *et al.* Green Synthesis of Metal Oxide Nanoparticles via Plant Extracts for Biological Applications: A Review. Trends Sci. 2025;22(6). https://doi.org/10.48048/tis.2025.9592.
4. Wang ZL. ZnO nanowire and nanobelt platform for nanotechnology. Mater Sci Eng R Rep. 2009;64(3-4):33-71. https://doi.org/10.1016/j.mser.2009.02.001.
5. Mohamad Sukri SNA, Shameli K, Mei-Theng Wong M, Teow S-Y, Chew J, Ismail NA. Cytotoxicity and antibacterial activities of plant-mediated synthesized zinc oxide (ZnO) nanoparticles using Punica granatum (pomegranate) fruit peels extract. J Mol Struct. 2019;1189:57-65. https://doi.org/10.1016/j.molstruc.2019.04.026.
6. Darezereshki E, Alizadeh M, Bakhtiari F, Schaffie M, Ranjbar M. A novel thermal decomposition method for the synthesis of ZnO nanoparticles from low concentration $ZnSO_4$ solutions. Appl Clay Sci. 2011;54(1):107-11. https://doi.org/10.1016/j.clay.2011.07.023.
7. Tari O, Aronne A, Addonizio ML, Daliento S, Fanelli E, Pernice P. Sol–gel synthesis of ZnO transparent and conductive films: A critical approach. Sol Energy Mater Sol Cells. 2012;105:179-86. https://doi.org/10.1016/j.solmat.2012.06.016.
8. Hayat K, Gondal M, Khaled MM, Ahmed S, Shemsi AM. Nano ZnO synthesis by modified sol-gel method and its application in heterogeneous photocatalytic removal of phenol from water. Appl Catal A Gen. 2011;393(1-2):122-9. https://doi.org/10.1016/j.apcata.2010.11.032.
9. Ann LC, Mahmud S, Bakhori SKM, Sirelkhatim A, Mohamad D, Hasan H, *et al.* Antibacterial responses of zinc oxide structures against Staphylococcus aureus, Pseudomonas aeruginosa and Streptococcus pyogenes. Ceram Int. 2014;40(2):2993-3001. https://doi.org/10.1016/j.ceramint.2013.10.008.
10. Ashar A, Iqbal M, Bhatti IA, Ahmad MZ, Qureshi K, Nisar J, *et al.* Synthesis, characterization and photocatalytic activity of ZnO flower and pseudo-sphere: Nonylphenol ethoxylate degradation under UV and solar irradiation. J Alloys Compd. 2016;678:126-36. https://doi.org/10.1016/j.jallcom.2016.03.251.
11. Ata S, Shaheen I, Ghafoor S, Sultan M, Majid F, Bibi I, *et al.* Graphene and silver decorated ZnO composite synthesis, characterization and photocatalytic activity evaluation. Diam Relat Mater. 2018;90:26-31. https://doi.org/10.1016/j.diamond.2018.09.015.
12. Sangkhaprom N, Supaphol P, Pavarajarn V. Fibrous zinc oxide prepared by combined electrospinning and solvothermal techniques. Ceram Int. 2010;36(1):357-63. https://doi.org/10.1016/j.ceramint.2009.09.014.
13. Wang Y, Zhang C, Bi S, Luo G. Preparation of ZnO nanoparticles using the direct precipitation method in a membrane dispersion micro-structured reactor. Powder Technol. 2010;202(1-3):130-6. https://doi.org/10.1016/j.powtec.2010.04.027.
14. Jajarmi P. Fabrication of pure ZnO nanoparticles by polymerization method. Mater Lett. 2009;63(30):2646-8. https://doi.org/10.1016/j.matlet.2009.08.062.
15. Kim M, Osone S, Kim T, Higashi H, Seto T. Synthesis of nanoparticles by laser ablation: A review. KONA Powder Part J. 2017;34:80-90. https://doi.org/10.1016/j.matlet.2009.08.062.
16. Yadav VK, Ali D, Khan SH, Gnanamoorthy G, Choudhary N, Yadav KK, *et al.* Synthesis and characterization of amorphous iron oxide nanoparticles by the sonochemical method and their application for the remediation of heavy metals from wastewater. Nanomaterials. 2020;10(8):1551. https://doi.org/10.3390/nano10081551.

17. Mishra P, Yadav RS, Pandey AC. Growth mechanism and photoluminescence property of flower-like ZnO nanostructures synthesized by starch-assisted sonochemical method. Ultrason Sonochem. 2010;17(3):560-5. https://doi.org/10.1016/j.ultsonch.2009.10.017.
18. Hachem K, Ansari MJ, Saleh RO, Kzar HH, Al-Gazally ME, Altimari US, *et al.* Methods of chemical synthesis in the synthesis of nanomaterial and nanoparticles by the chemical deposition method: a review. BioNanoSci. 2022;12(3):1032-57. https://doi.org/10.1007/s12668-022-00996-w.
19. Wang R-C, Tsai C-C. Efficient synthesis of ZnO nanoparticles, nanowalls, and nanowires by thermal decomposition of zinc acetate at a low temperature. Appl Phys A. 2009;94:241-5. https://doi.org/10.1007/s00339-008-4755-0.
20. ÖNem E, Mert SİVrİ F, AkkoÇ S, ÇIrrik C, Ezer A. Biosynthesis of ZnO nanoparticles using Laurus nobilis leaf extract and investigation of antiproliferative and antibacterial activity potential. Int J Second Metab. 2023;10(3):414-24. https://doi.org/10.21448/ijsm.1266244.
21. Fardood ST, Ramazani A, Joo SW. Sol-gel synthesis and characterization of zinc oxide nanoparticles using black tea extract. J Appl Chem Res. 2017;11(4):8-17.
22. Sackey J, Nwanya A, Bashir A, Matinise N, Ngilirabanga J, Ameh A, *et al.* Electrochemical properties of Euphorbia pulcherrima mediated copper oxide nanoparticles. Mater Chem Phys. 2020;244:122714. https://doi.org/10.1016/j.matchemphys.2020.122714.
23. Naseer M, Aslam U, Khalid B, Chen B. Green route to synthesize Zinc Oxide Nanoparticles using leaf extracts of Cassia fistula and Melia azadarach and their antibacterial potential. Sci Rep. 2020;10(1):9055. https://doi.org/10.1038/s41598-020-65949-3.
24. Perveen R, Shujaat S, Qureshi Z, Nawaz S, Khan MI, Iqbal M. Green versus sol-gel synthesis of ZnO nanoparticles and antimicrobial activity evaluation against panel of pathogens. J Mater Res Technol. 2020;9(4):7817-27. https://doi.org/10.1016/j.jmrt.2020.05.004.
25. Saeid Taghavi Fardooda, Ali Ramazani, Farzaneh Moradniaa, Zolfa Afsharia, Sara Ganjkhanlua, Zarea FY. Green Synthesis of ZnO Nanoparticles via Sol-gel Method and Investigation of Its Application in Solvent-free Synthesis of 12-Aryl-tetrahydrobenzo[α]xanthene-11-one Derivatives Under Microwave Irradiation. Chem. Methodol. 2019;3(6):696-706. https://doi.org/10.33945/sami/chemm.2019.6.2.
26. Hamouda RA, Yousuf WE, Mohammed ABA, Darwish DB, Abdeen EE. Comparative Study Between Zinc Oxide Nanoparticles Synthesized By Dig J Nanomater Biostructures. 2020;15(1):93–106.
27. Dalmaz A, Kasımfırtına E, Sivrikaya Özak S. Green synthesis of ZnO nanoparticles using Laurus nobilis L. extract and investigation of corrosion inhibition properties of DES-based nanofluids. Journal of the J. Iran. Chem. Soc. 2024;21 (4):1101-12. https://doi.org/10.1007/s13738-024-02981-4.
28. ÖNem E, Mert SİVrİ F, AkkoÇ S, ÇIrrik C, Ezer A. Biosynthesis of ZnO nanoparticles using Laurus nobilis leaf extract and investigation of antiproliferative and antibacterial activity potential. International J Second Metab. 2023;10(3):414-24. https://doi.org/10.21448/ijsm.1266244.
29. Fakhari S, Jamzad M, Kabiri Fard H. Green synthesis of zinc oxide nanoparticles: a comparison. Green Chem Lett Rev. 2019;12(1):19-24. https://doi.org/10.1080/17518253.2018.1547925.
30. Shafiee P, Reisi Nafchi M, Eskandarinezhad S, Mahmoudi S, Ahmadi E. Sol-gel zinc oxide nanoparticles: advances in synthesis and applications. Synth Sinter 2021;1(4). https://doi.org/10.53063/synsint.2021.1477.
31. Mahdi Ismail SM, Ahmed SM, Abdulrahman AF, AlMessiere MA. Characterization of green synthesized of ZnO nanoparticles by using pinus brutia leaves extracts. J Mol Struct 2023;1280. https://doi.org/10.1016/j.molstruc.2023.135063.
32. Manikandan B, Endo T, Kaneko S, Murali KR, John R. Properties of sol gel synthesized ZnO nanoparticles. J Mater Sci Mater Electron 2018;29(11):9474-85. https://doi.org/10.1007/s10854-018-8981-8.
33. Chemingui H, Missaoui T, Mzali JC, Yildiz T, Konyar M, Smiri M, *et al.* Facile green synthesis of zinc oxide nanoparticles (ZnO NPs): antibacterial and photocatalytic activities. Mater Res Express. 2019;6(10). https://doi.org/10.1088/2053-1591/ab3cd6.
34. Ananya Barman TD, Ayush Khamrui, Arnab Basu. Review On Green Synthesis Of Zno Nano Particles And Their Applications. 2020.
35. Singh P, Kim Y-J, Zhang D, Yang D-C. Biological synthesis of nanoparticles from plants and microorganisms. Trends Biotechnol. 2016;34(7):588-99. https://doi.org/10.1016/j.tibtech.2016.02.006.
36. Alejo-Armijo A, Altarejos J, Salido S. Phytochemicals and biological activities of laurel tree (Laurus nobilis). Nat Prod Commun. 2017;12(5):1934578X1701200519. https://doi.org/10.1177/1934578X1701200519.
37. Remini H, Mazauric J, Madani K, Boulekbache-Makhlouf L. Phytochemical analysis and antioxidant activity of Eucalyptus globulus: A comparative study between fruits and leaves extracts. J Chem Eng Bioanal Chem. 2016;1:23-9.
38. Jayachandran A, Aswathy T, Nair AS. Green synthesis and characterization of zinc oxide nanoparticles using Cayratia pedata leaf extract. Biochem Biophys Rep. 2021;26:100995. https://doi.org/10.1016/j.bbrep.2021.100995.
39. Barzinjy AA, Azeez HH. Green synthesis and characterization of zinc oxide nanoparticles using Eucalyptus globulus Labill. leaf extract and zinc nitrate hexahydrate salt. SN Appl Sci. 2020;2(5):991. https://doi.org/10.1007/s42452-020-2813-1.
40. Norouzi R, Hejazy M, Ataei A. Scolicidal activity of zinc oxide nanoparticles against hydatid cyst protoscolices in vitro. Nanomed Res J. 2019;4(1):23-8. https://doi.org/10.22034/nmrj.2019.01.004.
41. Zandi S, Kameli P, Salamati H, Ahmadvand H, Hakimi M. Microstructure and optical properties of ZnO nanoparticles prepared by a simple method. Phys B Condens Matter. 2011;406(17):3215-8. https://doi.org/10.1016/j.physb.2011.05.026.
42. Pang X, Sellaoui L, Franco D, Dotto GL, Georgin J, Bajahzar A, *et al.* Adsorption of crystal violet on biomasses from pecan nutshell, para chestnut husk, araucaria bark and palm cactus: Experimental study and theoretical modeling via monolayer and double layer statistical physics models. Chem Eng J. 2019;378. https://doi.org/10.1016/j.cej.2019.122101.
43. Mahdi Ismail SM, Ahmed SM, Abdulrahman AF, AlMessiere MA. Characterization of green synthesized of ZnO nanoparticles by using pinus brutia leaves extracts. J Mol Struct. 2023;1280. https://doi.org/10.1016/j.molstruc.2023.135063.
44. Carofiglio M, Barui S, Cauda V, Laurenti M. Doped zinc oxide nanoparticles: synthesis, characterization and potential use in nanomedicine. Appl Sci. 2020;10(15):5194. https://doi.org/10.3390/app10155194.
45. Yakubu U, Tijjani Hassan D. Preparation and characterization of metal oxide nanofluids for solar thermal application. Dutse J Pure Appl Sci. 2025;11(3c):240-8. https://doi.org/10.4314/dujopas.v11i3c.23.

46. Jagadeeswar V, Dhinesh V, Roopan SM, Samuel EJJ. Plant Extract-Mediated Synthesis of Ag-Doped ZnO: Eco-Friendly Nanomaterial for Environmental Restoration, Microbial Inhibition, Cell Toxicity, Antioxidant Potential, and Sensing. Colloid J. 2023;85(5):827-45. https://doi.org/10.1134/S1061933X23600513.
47. Modwi A, Ali MKM, Taha KK, Ibrahem MA, El-Khair HM, Eisa MH, *et al.* Structural and optical characteristic of chalcone doped ZnO nanoparticles. J Mater Sci: Mater Electron. 2017;29(4):2791-6. https://doi.org/10.1007/s10854-017-8207-5.
48. Alias SS, Ismail AB, Mohamad AA. Effect of pH on ZnO nanoparticle properties synthesized by sol–gel centrifugation. J Alloys Compd. 2010;499(2):231-7. https://doi.org/10.1016/j.jallcom.2010.03.174.
49. Vafaee M, Ghamsari MS. Preparation and characterization of ZnO nanoparticles by a novel sol–gel route. Mater Lett. 2007;61(14-15):3265-8. https://doi.org/10.1016/j.matlet.2006.11.089.
50. Wang M, Wang J, Chen W, Cui Y, Wang L. Effect of preheating and annealing temperatures on quality characteristics of ZnO thin film prepared by sol–gel method. Mater Chem Phys. 2006;97(2-3):219-25. https://doi.org/10.1016/j.molstruc.2024.137820.
51. Alam MK, Hossain MS, Bahadur NM, Ahmed S. A comparative study in estimating of crystallite sizes of synthesized and natural hydroxyapatites using Scherrer Method, Williamson-Hall model, Size-Strain Plot and Halder-Wagner Method. J Mol Struct. 2024;1306:137820. https://doi.org/10.1016/j.molstruc.2024.137820.
52. Ebrahim M, Saffour Z. Synthesis and Characterization of ZnO Nanoparticles and Their Application on Cotton Fabrics to Obtain Superhydrophobic Surfaces. Baghdad Sci J. 2024;21(8). https://doi.org/10.21123/bsj.2024.8934.
53. Dalmaz A, Kasımfırtına E, Sivrikaya Özak S. Green synthesis of ZnO nanoparticles using Laurus nobilis L. extract and investigation of corrosion inhibition properties of DES-based nanofluids. J Iran Chem Soc. 2024;21(4):1101-12. https://doi.org/10.1007/s13738-024-02981-4.
54. Singh A, Singh N, Hussain I, Singh H, Yadav V, Singh S. Green synthesis of nano zinc oxide and evaluation of its impact on germination and metabolic activity of Solanum lycopersicum. J Biotechnol. 2016;233:84-94. https://doi.org/10.1016/j.jbiotec.2016.07.010.
55. Sundrarajan M, Ambika S, Bharathi K. Plant-extract mediated synthesis of ZnO nanoparticles using Pongamia pinnata and their activity against pathogenic bacteria. Adv Powder Technol. 2015;26(5):1294-9. https://doi.org/10.1016/j.apt.2015.07.001.
56. Perveen R, Shujaat S, Qureshi Z, Nawaz S, Khan MI, Iqbal M. Green versus sol-gel synthesis of ZnO nanoparticles and antimicrobial activity evaluation against panel of pathogens. J Mater Res Technol. 2020;9(4):7817-27. https://doi.org/10.1016/j.jmrt.2020.05.004.

تحضير ودراسة خصائص جسيمات أكسيد الزنك النانوية: من الطرق الكيميائية إلى الطرق الخضراء

كاوة سعيد سليمان ، ايوب صابر كريم

القسم الفيزياء ، الكلية تربية ، الجامعة صلاح الدين-اربيل ، اربيل ، عراق

الخلاصة

استخدمت هذه الدراسة جسيمات أكسيد الزنك النانوية (ZnO NPs) التي تم تحضيرها بطريقتين منفصلتين: التركيب الأخضر (الحيوي) وطريقة السول-جل. حيث تم في الطريقة الخضراء استخدام مستخلص أوراق نبات الغار (Laurus Nobilis). تم تقييم الجسيمات النانوية الناتجة من كلا الطريقتين باستخدام تقنيات متعددة تشمل: الطيف المرئي فوق البنفسجي (UV-visible)، وتحليل الأشعة تحت الحمراء بالتحويل فورييه (FTIR)، وحيود الأشعة السينية (XRD)، وتحليل طيف الطاقة المشتتة للأشعة السينية (EDX)، ومجهر الانبعاث الماسح الإلكتروني الميداني (FESEM) . أظهرت النتائج نجاح تحضير جسيمات أكسيد الزنك النانوية بكلا الطريقتين (السول-جل والتركيب الأخضر). كشفت أنماط حيود الأشعة السينية (XRD) بنية بلورية سداسية من نوع الورتزيت، بمتوسط حجم بلوري قدره **18.46 نانومتر** للطريقة الخضراء و**25.77 نانومتر** لطريقة السول-جل، مع وجود قمم واضحة للأكسجين والزنك مما يدل على طبيعة البلورية العالية. كما تم استخدام مطيافية الأشعة فوق البنفسجية لدراسة الخصائص البصرية، حيث بلغت فجوة النطاق الطاقة المتوسطة **2.81 إلكترون فولت** للجسيمات المحضرة بالطريقة الخضراء و**2.84 إلكترون فولت** لطريقة السول-جل. أكدت نتائج تحليل EDX على نقاء عالٍ لجسيمات أكسيد الزنك النانوية المحضرة بكلا الطريقتين، حيث كانت نسبة الزنك **81%** والأكسجين **19%** في الطريقة الخضراء، بينما كانت **80.9%** زنك و**19.1%** أكسجين في طريقة السول-جل. كما أظهرت صور FESEM أن الجسيمات النانوية الناتجة عن الطريقة الخضراء اتخذت شكلاً كروياً، في حين ظهرت على شكل حبيبات نانوية أو أسطوانية (Nano rice/rod) في طريقة السول-جل. بلغ متوسط حجم الجسيمات **151 نانومتر** للطريقة الخضراء و**173 نانومتر** لطريقة السول-جل. هذا العمل يقدم مقارنة فعالة بين طريقتين مختلفتين لتحضير الجسيمات النانوية، مما يسلط الضوء على الخصائص المتميزة لكل منهما..

الكلمات المفتاحية: جسيمات نانوية من أكسيد الزنك، تحضير أخضر، ورقة غار , طريقة سول-جل، توصيف نانوي.